iJRASET
International Journal For Research in Applied Science and Engineering Technology

INTERNATIONAL JOURNAL FOR RESEARCH

IN APPLIED SCIENCE & ENGINEERING TECHNOLOGY

Volume: 7 **Issue:** VI **Month of publication:** June 2019

DOI: http://doi.org/10.22214/ijraset.2019.6008

www.ijraset.com

Call: 08813907089 | E-mail ID: ijraset@gmail.com

International Journal for Research in Applied Science & Engineering Technology (IJRASET)
ISSN: 2321-9653; IC Value: 45.98; SJ Impact Factor: 7.177
Volume 7 Issue VI, Jun2019- Available at www.ijraset.com

Kinematic and Dynamic Analysis of an Upper limb Rehabilitation Robot

Kalewar Amol[1], Dr. G. Satish Babu[2]
[1]P.G Student, [2]Professor, Department of Mechanical Engineering
JNTUH College of Engineering, Kukatpally, Hyderabad, India

Abstract: ***The system outputs are predictable using the model, knowledge of an accurate model of a system is always beneficial to develop a robust and safe control while allowing a reduction of sensors-related costs. This paper presents the kinematic and dynamic analysis of multipurpose upper limb rehabilitation robot, Universal Haptic Pantograph. This robot, due to its lockable and un-lockable joints, can change its mechanical structure so that it empowers stroke patients to perform diverse training activities, exercises of the shoulder, elbow, and wrist. This work centers around the ARM mode, which is a preparation mode used to restore elbow and shoulder. The kinematical model of UHP is recognized based on the loop vector conditions, while the dynamical model is inferred dependent on the Lagrangian Formulation. The test outcomes show that the mean position error between the estimated values with the robot and actual measured values stays in 2mm. Moreover, the error between the estimated and measured interaction force is smaller than 10% of the maximum force range. So the robot can be adapted to estimate motion and force as well as control it without the need for additional sensors such as force sensor, resulting in the reduction of total robot cost.***

Keywords: Upper limbs rehabilitation, Rehabilitation robot , Kinematic Analysis, Dynamic Analysis

1. INTRODUCTION

These days, more than 33 million individuals in the world are influenced by strokes. State-of-the-art, different research results on stroke have exhibited that, because of brain plasticity, stroke patients may recoup the greater part of their aptitudes executing sufficient recovery works out. Be that as it may, in traditional recovery programs, stroke patients require steady supervision by the specialist, which increases the financial expense of the treatment, and prompts the decrease of rehabilitation times, hindering constant and long haul restoration mediations. Thus, in the course of the most recent few decades, a few rehabilitation robotic devices for stroke patients, especially for upper limbs rehabilitation, have been developed and exhibited at both academic and clinical settings. The robots are accepted to be a decent option in contrast to conventional recovery treatments because of a few favourable circumstances of the robot-interceded treatment: 1) robots imitate and repeat the developments delivered by a physiotherapist, executing longer span, higher recurrence and better precision treatments; 2) with the target of assessing the advancement of the patient and additionally adjusting the activities to their necessities, the device can go about as an estimation instrument that measures powers as well as developments; 3) utilizing a graphical interface, an virtual reality condition can be manufactured, encouraging patient association in the rehabilitation procedure.

Consequently, an appropriate and exact mathematical model of the robot not just encourages the plan of the propelled control methodologies yet in addition potentially acknowledges reasonable mechanical answers for rehabilitation zone. In this specific situation, this examination displays the kinematical and dynamical demonstrating approach and the resultant models of a multipurpose upper limb rehabilitation robot, alluded to as the Universal Haptic Pantograph (UHP). The UHP is a Pantograph based innovative device impelled by two SEAs (Series Elastic Actuator) whose primary trademark is the re-configurability of its mechanical structure utilizing lockable/un-lockable joints. This element permits to adjust the structure to the rehabilitation needs of various parts of the upper limbs.

II. UNIVERSAL HAPTIC PANTOGRAPH

The Universal Haptic Pantograph (UHP) is a rehabilitation robot created to prepare impaired upper limbs after a stroke. A standout amongst the most essential advantages of the UHP is its re-configurability, which permits to change its mechanical structure on account of its lockable / un-lockable joints. Along these lines, for each mechanical setup, the UHP can execute distinctive sorts of exercises that attention on specific parts of the upper limb: the shoulder, elbow and wrist. This work centers in a standout amongst the most entire modes, the ARM mode. This mode is utilized to rehabilitate elbow and shoulder by means of 2 degrees of freedom (DOF) motions that permit arm extension in forward, backward, leftward and rightward directions. So as to provide this movement, a Pantograph-based structure is utilized to interact with the patient. The Pantograph is actuated by two perpendicular SEAs (Series Elastic Actuator) so as to generate forces in *x* and y directions. The motion of the UHP results from the forces (F_{Cn}) applied by the user in the

contact point (P_{Cn}) and the torques ($\boldsymbol{\tau_m}$) applied by the motors through the SEA based drive system. The two subsystems are connected in the transmission point (P_T) with the end goal that the torque ($\boldsymbol{\tau_m}$) exerted by the actuators of the drive system and the force (F_{Cn}) and motion (P_{Cn}) applied to the Pantograph by the patient are transmitted bilaterally in the form of force (F_T) and motion (P_T). As referenced previously, an appropriate mathematical model of the robot is required to actualize the robot-patient force interaction controller. Since the model requests position measurements of the drive system for the estimation of the torque ($\boldsymbol{\tau_m}$), the force (F_{Cn}) and motion (P_{Cn}), the UHP prototype includes two optical encoders and two linear potentiometers to measure the actuators rotation angle (q_m) and the lengths of SEAs upper springs (n_{S_A} and n_{S_B}), respectively. The model of the SEA based drive framework is utilized to register the actuators torque ($\boldsymbol{\tau_m}$) in the force controller as well as to assess the force (F_T) and motion (P_T) of the transmission point. The Pantograph model, on the other hand, estimates the force (F_{Cn}) and motion (P_{Cn})applied by the patient. The two models will be described in chapter 3.

III. KINEMATIC AND DYNAMIC MODELS

A. *In this section UHP Kinematic and Dynamic Models are Presented*

1) *Kinematic Model of SEA :* To infer the kinematical model of SEA based drive framework, spring variable lengths ($\boldsymbol{n_S}$) and the estimations of the reliant factors ($\boldsymbol{q_{na_S}}$) will be determined in terms of the rotation angles of the motors ($\boldsymbol{q_m}$).

$$I_A + P_A - P_T = 0 \rightarrow I_A = \begin{bmatrix} x_T \\ y_T \\ z_T \end{bmatrix} - \begin{bmatrix} x_A \\ 0 \\ z_A \end{bmatrix}$$

$$I_B + P_B - P_T = 0 \rightarrow I_B = \begin{bmatrix} x_T \\ y_T \\ z_T \end{bmatrix} - \begin{bmatrix} 0 \\ y_B \\ z_B \end{bmatrix} \quad (1)$$

From Eq. (1) , the relationship between the lengths $l_A$and l_B and the transmission point displacement $P_T = ([x_T \quad y_T \quad z_T]^T)$ can be formulated by

$$l_A = |I_A| = \sqrt{(x_T - x_A)^2 + y^2{}_T + (z_T - z_A)^2}$$

$$l_B = |I_B| = \sqrt{x^2{}_T + (y_T - y_B)^2 + (z_T - z_B)^2} \quad (2)$$

On the other hand, the relationship between the upper cable length $l_A$and $l_B$and the measurable upper spring lengths $n_{S_A}$and n_{S_B}can be defined in terms of the rotation angle of each motor $\boldsymbol{q_{m_i}}$

$$n_{S_A} = l_A + (q_{m1} - \theta_A)r_{p1} - l_1$$

$$n_{S_B} = l_B + (q_{m2} - \theta_B)r_{p1} - l_1 \quad (3)$$

Where l_1 is the distance between the equilibrium point (P_0) to actuated pulley (p_1), r_{p_1} is the radius of actuated pulleys, and the $\theta_A$and θ_B are derived as

$$\theta_A = arctan\left(\frac{x_A + l_1}{z_A + r_{p1}}\right)$$

$$\theta_B = arctan\left(\frac{y_B - l_1}{z_B + r_{p1}}\right) \quad (4)$$

Therefore, combining Eqs. (2) and (3) yield

$$n_{S_A} - q_{m1}r_{p1} = \sqrt{(x_T - x_A)^2 + y^2{}_T + (z_T - z_A)^2} - \theta_A r_{p1} - l_1$$

$$n_{S_B} - q_{m2}r_{p1} = \sqrt{x^2{}_T + (y_T - y_B)^2 + (z_T - z_B)^2} - \theta_B r_{p1} - l_1 \quad (5)$$

In any case, as P_T has three variables (x_T, y_T and z_T), a third equation is required to illuminate the P_T. The third equation can be acquired by analyzing the motion of the Pantograph actuated bar. The actuated bar shows a spherical joint P_E with respect to the Fixed structure .Consequently, the motion of P_T is constrained to the surface of a sphere of radius l_3

$$x^2{}_T + y^2{}_T + (l_3 - z_T)^2 = l_3{}^2 \tag{6}$$

After solving the P_T, the estimation of lengths n_{S_C} and n_{S_D} is to be calculated. For that reason, a similar strategy as that employed in the past area is applied.

$$P_C + I_C - P_T = 0 \rightarrow I_C = \begin{bmatrix} x_T \\ y_T \\ z_T \end{bmatrix} - \begin{bmatrix} x_C \\ 0 \\ z_C \end{bmatrix}$$

$$P_D + I_D - P_T = 0 \rightarrow I_D = \begin{bmatrix} x_T \\ y_T \\ z_T \end{bmatrix} - \begin{bmatrix} 0 \\ y_D \\ z_D \end{bmatrix} \tag{7}$$

$$l_C = |I_C| = \sqrt{(x_T - x_C)^2 + y^2{}_T + (z_T - z_C)^2}$$

$$l_D = |I_D| = \sqrt{x^2{}_T + (y_T - y_D)^2 + (z_T - z_D)^2} \tag{8}$$

So, the variable length of un-sensored springs is

$$n_{S_C} = l_C - q_{m1} r_{p1} + \theta_C r_{p2} - l_2$$

$$n_{S_D} = l_D - q_{m2} r_{p1} + \theta_D r_{p2} - l_2 \tag{9}$$

2) Dynamic Model of the Actuators: Once the variable lengths(n_S) of the springs and the dependent variables (q_{nas})are calculated, the dynamical model of the motor can be obtained from the spring forces that are transmitted through the cables. The magnitude of each spring force (F_{S_i}) relies upon its variable length (n_{S_i}) and its constant (k_{S_i}), while its direction (u_i) depends on the passive variables (q_{nas})

$$F^m{}_{S_i}(n_{S_i}, q_{nas}) = F_{S_i} u_i = k_{S_i} n_{S_i} u_i \tag{10}$$

where u_i is the unitary force direction vectors

So, the torques exerted by the springs in each motor is

$$\tau_{S_1} = \tau_{S_A} + \tau_{S_C} = k_{S_A} n_{S_A} r_{p1} \sqrt{cos^2\beta_A cos^2\delta_A + sin^2\delta_A} + k_{S_C} n_{S_C} r_{p1}$$

$$\tau_{S_2} = \tau_{S_B} + \tau_{S_D} = k_{S_B} n_{S_B} r_{p1} \sqrt{cos^2\beta_B cos^2\delta_B + sin^2\delta_B} + k_{S_D} n_{S_D} r_{p1} \tag{11}$$

As the drive framework depends on a motor-spring actuation, the applied force ($\mathbf{F_T}$) is determined based on the spring forces that are transmitted through the cables $\mathbf{F^T{}_{S_i}}$

$$\mathbf{F_T} = \sum_{i=A}^{D} \mathbf{F^T{}_{S_i}} = \mathbf{F^T{}_{S_A}} + \mathbf{F^T{}_{S_B}} + \mathbf{F^T{}_{S_C}} + \mathbf{F^T{}_{S_D}} \tag{12}$$

B. Pantograph Structure

In this section kinematic and dynamic structure of pantograph is presented.

1) Kinematical Model : First, the Pantograph kinematical model, that relates the motion of the transmission point $P_T = [x_T \quad y_T \quad z_T]^T$, and the contact point position $P_{Cn} = [x_{Cn} \quad y_{Cn} \quad z_{Cn}]^T$ are determined dependent on the kinematical loop equation

$$P_T + I_5 + d_1 + I_7 - P_{Cn} = 0 \tag{13}$$

Solving for P_{Cn},

$$\begin{bmatrix} x_{Cn} \\ y_{Cn} \\ z_{Cn} \end{bmatrix} = \begin{bmatrix} x_T \\ y_T \\ z_T \end{bmatrix} + \frac{l_5 + d_1 + l_7}{l_3} \begin{bmatrix} -x_T \\ -y_T \\ l_3 - z_T \end{bmatrix}$$

$$= \frac{-l_4 - d_1 - l_7}{l_3} \begin{bmatrix} x_T \\ y_T \\ z_T \end{bmatrix} + \begin{bmatrix} 0 \\ 0 \\ l_5 + d_1 + l_7 \end{bmatrix} \quad (14)$$

Henceforth, derivating Eq. (14) , the input-output Jacobian can be determined

$$\dot{\mathbf{P}}_{\mathbf{Cn}} = \underbrace{\mathbf{J}_{\mathbf{x}}}_{\mathbf{3\times3}} \dot{\mathbf{P}}_{\mathbf{T}} \quad (15)$$

2) *Dynamic Model of Pantograph:* The dynamical model of the Pantograph is used to decide the relationship between the transmission ($\mathbf{F_T}$) and the contact force ($\mathbf{F_{Cn}}$) contingent upon the transmission motion ($\mathbf{P_T}$). For this reason, the Lagrangian formulation is used. In ARM mode the Pantograph is formed by five elements ($\mathbf{E_1}$, $\mathbf{E_2}$, $\mathbf{E_3}$, $\mathbf{E_4}$and $\mathbf{E_5}$), where $\mathbf{E_1}$, $\mathbf{E_2}$, $\mathbf{E_3}$have the similar motion due to the lockable joints $\mathbf{P_F}$). Therefore, the Langrangian function can be characterized as

$$\mathbf{L} = \mathbf{K_{E_1}} + \mathbf{K_{E_2}} + \mathbf{K_{E_3}} + \mathbf{K_{E_4}} + \mathbf{K_{E_5}} - (\mathbf{U_{E_1}} + \mathbf{U_{E_2}} + \mathbf{U_{E_3}} + \mathbf{U_{E_4}} + \mathbf{U_{E_5}}) \quad (16)$$

Where $\mathbf{K_{E_i}}$and $\mathbf{U_{E_i}}$are kinetic and potential energies of each element, defined as

$$\mathbf{K_{E_i}} = \frac{1}{2} m_{E_i} v_{CM_{E_i}}{}^T v_{CM_{E_i}} + \frac{1}{2} \omega_{CM_{E_i}}{}^T I_{E_i} \omega_{CM_{E_i}} \quad (17)$$

$$\mathbf{U_{E_i}} = m_{E_i} g\, h_{CM_{E_i}} \quad (18)$$

Where $m_{E_i}$is the mass of each element, I_{E_i}its inertia, $h_{CM_{E_i}}$the z co-ordinate of the center of mass position, $v_{CM_{E_i}}$the linear velocity of the center of mass and $\omega_{CM_{E_i}}$its angular velocity.

Applying the Lagrangian formulation (Eq. (16))

$$\mathbf{D_T}\ddot{\mathbf{P}}_{\mathbf{T}} + \mathbf{C_T}\dot{\mathbf{P}}_{\mathbf{T}} + \mathbf{G_T} = \frac{d}{dt}\left(\frac{\partial \mathbf{L}}{\partial \dot{\mathbf{P}}_{\mathbf{T}}}\right) - \frac{\partial \mathbf{L}}{\partial \mathbf{P_T}}$$

$$= \sum \boldsymbol{\lambda_T} \frac{\partial \Gamma_{\mathbf{T}}(\mathbf{P_T}, \mathbf{q_{na_A}})}{\partial \mathbf{P_T}} + \mathbf{F_T} \quad (19)$$

$$\mathbf{D_q}\ddot{\mathbf{q}}_{\mathbf{na_A}} + \mathbf{C_q}\dot{\mathbf{q}}_{\mathbf{na_A}} + \mathbf{G_q} = \frac{d}{dt}\left(\frac{\partial \mathbf{L}}{\partial \dot{\mathbf{q}}_{\mathbf{na_A}}}\right) - \frac{\partial \mathbf{L}}{\partial \mathbf{q}_{\mathbf{na_A}}}$$

$$\sum \boldsymbol{\lambda_T} \frac{\partial \Gamma_{\mathbf{T}}(\mathbf{P_T}, \mathbf{q_{na_A}})}{\partial \mathbf{q}_{\mathbf{na_A}}} \quad (20)$$

Where, $\Gamma_{\mathbf{T}}(\mathbf{P_T}, \mathbf{q_{na_A}}) = \mathbf{0}$ is the closure equation that relates the input and output factors (Eq. (14)), $\boldsymbol{\lambda_T}$ is the arrangement of Lagrange multipliers, and $\mathbf{F_T}$is the force applied in the transmission point ($\mathbf{P_T}$). On the other hand, inertia **D,** Coriolis **C** and gravity **G** terms, which relies on the reliable factors ($\mathbf{D_q}$, $\mathbf{C_q}$and$\mathbf{G_q}$) or transmission motion ($\mathbf{D_T}$, $\mathbf{C_T}$ and $\mathbf{G_T}$), can be effortlessly characterized by gathering acceleration, velocity and gravitational terms.

If the model is to be characterized in terms of $\mathbf{P_T}$, and considering that

$\mathbf{J}_{\mathbf{q_{na_A}}} = \partial \mathbf{q}_{\mathbf{na_A}} / \partial \mathbf{P_T}$

$$\mathbf{F_T} = \mathbf{D}\ddot{\mathbf{P}}_{\mathbf{T}} + \mathbf{C}\dot{\mathbf{P}}_{\mathbf{T}} + \mathbf{G} + \mathbf{F_E} \quad (21)$$

Where,

$$\mathbf{D} = \mathbf{D_T} + \mathbf{J_{q_{na_A}}}^T \mathbf{D_q} \mathbf{J_{q_{na_A}}}$$

$$\mathbf{C} = \mathbf{C_T} + \mathbf{J_{q_{na_A}}}^T \mathbf{C_q} \mathbf{J_{q_{na_A}}} + \mathbf{J_{q_{na_A}}}^T \mathbf{D_q} \dot{\mathbf{J}}_{\mathbf{q_{na_A}}}$$

$$\mathbf{G} = \mathbf{G_T} + \mathbf{J_{q_{na_A}}}^T \mathbf{G_q}$$

$$\mathbf{F_E} = -\mathbf{J_x}^T \mathbf{F_{Cn}} \quad (22)$$

In this manner the connection between the interaction force (F_{Cn}) and dynamical behavior (F_T and P_T) of the transmission point is acquired by Eq. (22) .

IV. RESULTS

Few tests were carried out to validate the kinematical and dynamical models of UHP rehabilitation robot, and that only the most significant results are shown to demonstrate the validity of the models. First, the kinematical models of the Pantograph in ARM mode were validated. For this purpose, the motors executed a 5s period sinusoidal motion without external force. This means that the user did not execute any resistive force to the movement of the motors. The motor rotation angles($\mathbf{q_m}$) and variable length of the upper springs ($n_{S_A}$and n_{S_B}were used to estimate the contact motion ($\mathbf{P_{Cn}}$). In order to validate the estimation, $\mathbf{P_{Cn}}$was also calculated from the inclinometer measurements.

Table1: Parameters of the UHP

Parameter	Value	Parameter	Value
l_1	0.575m	l_{10}	0.27
l_2	0.15m	m_{E_1}	0.882kg
l_3	0.18m	m_{E_2}	1.20kg
l_4	0.46m	m_{E_3}	1.15kg
l_5	0.65	m_{E_4}	1.50 kg
l_6	0.20	I_{m_1}	0.003615Ns^2/rad
l_7	0.13	I_{m_2}	0.002742Ns^2/rad
l_8	0.25	F_{c_1}	0.8404Nm
l_9	0.65	F_{c_2}	0.7312Nm

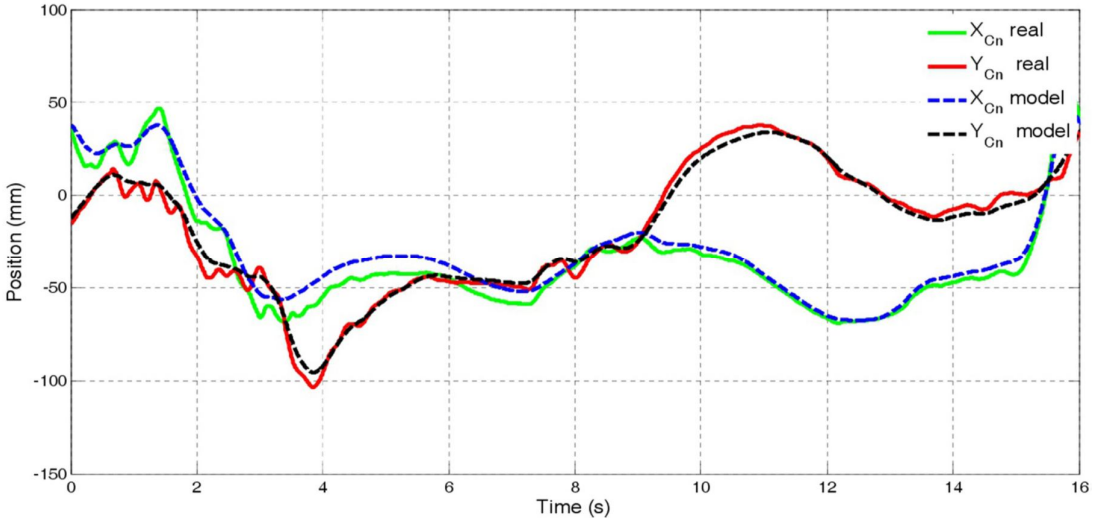

Fig.1. Kinematic analysis results of UHP

In Fig. 1, the real and estimated values of $\mathbf{P_{Cn}}$ are observed. As it can be extracted from the data, the mean error is smaller than 3 mm and the maximum error is 10 mm. As mentioned previously, motion area of the UHP in ARM mode is a circumference of 150 mm radius, hence, the motion error is less than 3.34% of the motion area.

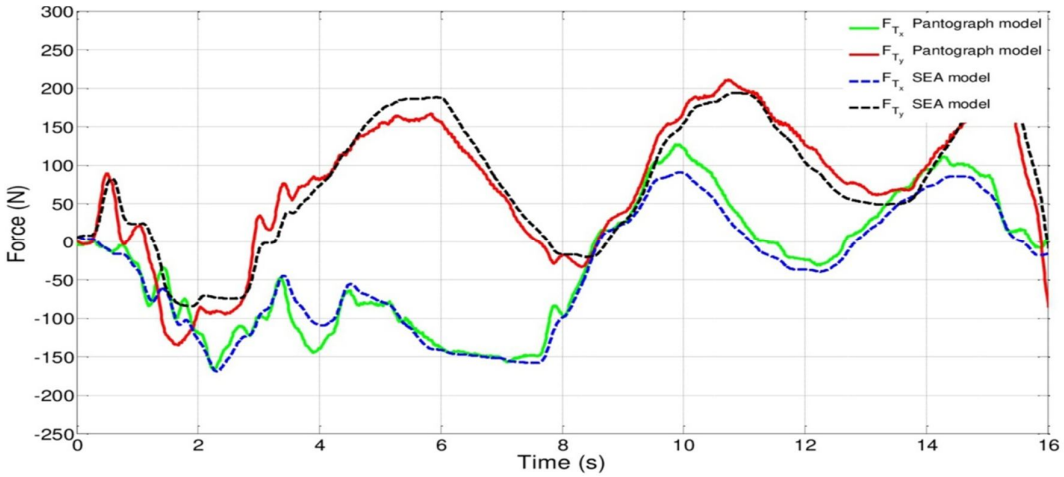

Fig.2. Dynamic analysis results of UHP

Fig.2, shows the values of $\mathbf{F_T}$ calculated with Pantograph in ARM mode. As it can be seen, the mean error is smaller than 10% of the maximum force range.

It is noticed that in health and care applications, for example, rehabilitation, movement precision isn't as basic as in different applications like surgery. The position resolution that sound people can control amid upper limbs movements is 5 mm in the normal, demonstrating that the mean error of 3 mm is higher than the resolution of human arm movement. In addition, in the large portion of genuine robot interceded trainings utilizing force, the force magnitude is smaller than 20 N for the patient safety, which means force errors of 10% compare to 2N. In this sense, the position and force errors acquired in this investigation are probably going to be adequate in the utilization for rehabilitation purpose.

V. CONCLUSIONS

In this paper, kinematic and dynamic analysis of the upper limb rehabilitation robot, Universal Haptic Pantograph (UHP) have been determined. This work centers around the ARM mode which is utilized for impaired elbow and shoulder rehabilitation, among various rehabilitation modes offered by UHP on account of its reconfigurable mechanical structure. The UHP structure can be isolated in two subsystems: a SEA based drive framework, and a Pantograph structure with which the patient connects. These two subsystems are associated through the transmission point, permitting the control of motion and force of UHP relying upon the purpose behind the recovery program. Based on the loop vector conditions and the Lagrangian definition, the kinematic and dynamic models of the two subsystems have been determined, intending to assess system outputs with the minimum of required sensors just as encourage the design of advanced interaction controllers between patient and UHP. For the approval, the system outputs assessed utilizing the models were contrasted and those gotten by estimations. The outcomes show that the motion mean error in the contact point ($\mathbf{P_{Cn}}$) is under 4% of the motion area, while the transmission power ($\mathbf{F_T}$) error is less than the 10% of maximum force range. Also, these outcomes suggest that the models can be utilized in the estimation of the system outputs just as in the design of the controller with adequate exactness and reliability for rehabilitation applications as the acquired precision is higher than human motion and force resolution. Along these lines, it is concluded that the utilization of the created model can limit required sensor sets, bringing about the decrease of the robot cost. In future works, the proposed kinematic and dynamic models will apply to the execution advanced controllers for rehabilitation purpose. Also, the control execution will be compared with that dependent on direct measurement of force and motion while interacting with the patient.

REFERENCES

[1] J.L. Pons, R. Raya, J. González, Emerging Therapies in Neuro rehabilitation II, in: Biosystems & Biorobotics, 10, Springer International Publishing, Cham, 2016, pp. 29–64,

[2] L. Sawaki, Use-dependent plasticity of the human motor cortex in health and disease, IEEE Eng. Med. Biol. Mag. 24 (1) (2005) 36–39.

[3] N. Norouzi-Gheidari, P.S. Archambault, J. Fung, Effects of robot-assisted therapy on stroke rehabilitation in upper limbs: systematic review and meta-analysis of the literature, J. Rehabil. Res. Dev. 49 (4) (2012) 479–495.

[4] N. Jarrassé, T. Proietti, V. Crocher, J. Robertson, A. Sahbani, G. Morel, A. Roby- Brami, Robotic exoskeletons: a perspective for the rehabilitation of arm coordination in stroke patients, Front. Hum. Neurosci. 8 (947) (2014) 1–13.

[5] R. Vertechy, A. Frisoli, A. Dettori, M. Solazzi, M. Bergamasco, Development of a new exoskeleton for upper limb rehabilitation, IEEE International Conference on Rehabilitation Robotics, 2009, pp. 188–193.

[6] M.H. Rahman, M.J. Rahman, O.L. Cristobal, M. Saad, J.P. Kenné, P.S. Ar-chambault, Development of a whole arm wearable robotic exoskeleton for rehabilitation and to assist upper limb movements, Robotica 33 (2014) 19–39.

[7] Z. Song, S. Zhang, B. Gao, Implementation of resistance training using an upper-limb exoskeleton rehabilitation device for elbow joint, J. Med. Biol. Eng. 34 (2) (2013) 188–196.

[8] K. Kiguchi, Y. Hayashi, An EMG-based control for an upper-limb power-assist exoskeleton robot, IEEE Trans. Syst. Man Cybern. 42 (4) (2012) 1064–1071.

[9] N. Hogan, Impedance control: an approach to manipulation: part i theory, J. Dyn. Syst. Meas. Control 107 (1985) 1–27.

[10] M. Babaiasl, S.H. Mahdioun, P. Jaryani, M. Yazdani, A review of tech- nological and clinical aspects of robot-aided rehabilitation of upper- extremity after stroke, Disabil. Rehabil.: Assist. Technol. 11 (2015) 263–280

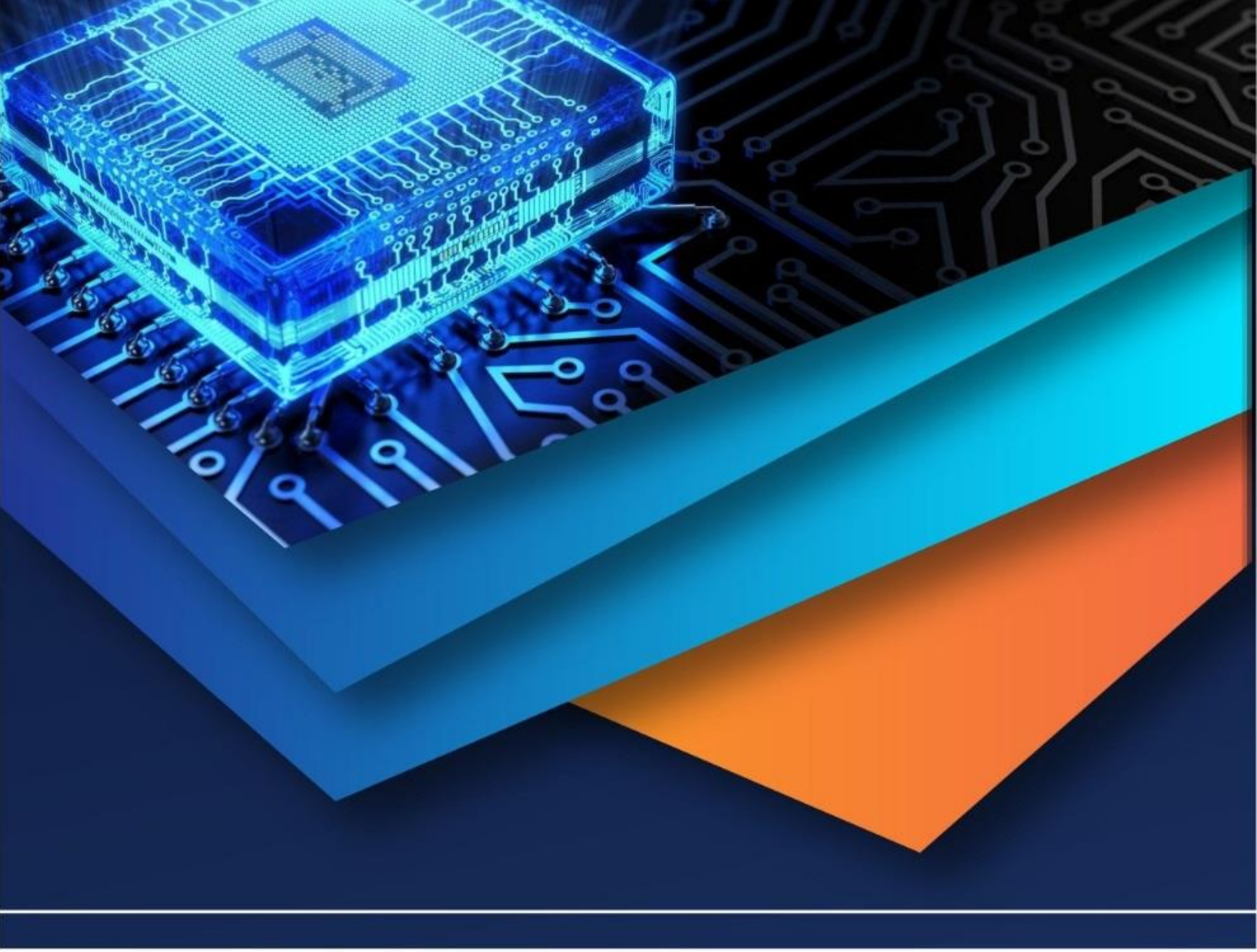

10.22214/IJRASET

45.98

IMPACT FACTOR: 7.129

IMPACT FACTOR: 7.429

INTERNATIONAL JOURNAL FOR RESEARCH

IN APPLIED SCIENCE & ENGINEERING TECHNOLOGY